DOI: 10.1002/ejoc.200700932

Cyclotetrapeptide Mimics Based on a 13-Membered, Partially Modified Retro-Inverso Structure

Luca Gentilucci,*[a] Giuliana Cardillo,[a] Alessandra Tolomelli,[a] Santi Spampinato,[b] Antonino Sparta,[b] and Federico Squassabia[a]

Keywords: Medicinal chemistry / Inhibitors / Peptidomimetics / Conformation analysis / Cell adhesion

Cyclic tetrapeptides (CTP) incorporating a distinct β-amino acid represent realistic conformationally homogeneous CTP analogs, and they can find application in medicinal chemistry as turn mimics and scaffolds. In this respect, we synthesized a small library of CTP-mimics based on a 13-membered, partially modified retro-inverso (PMRI) structure containing a 1,2-diamine as a β-amino acid mimetic and malonic acid as a glycine surrogate. Conformational analysis revealed that the PMRI–CTP models containing an unsubstituted diamine (**1**, **2**) exhibited a certain flexibility. On the contrary, the introduction of a chiral, substituted 1,2-diamine rendered the backbone more rigid (**3**, **4**) and induced type I β-turn structures. The comparison with a β-amino acid containing CTP revealed that the PMRI–CTPs can be regarded as alternative β-turn scaffolds. To validate the structural deductions based on conformational analysis, we synthesized a couple of diastereomeric RGD analogs (**5**, **6**) as integrin inhibitors, and we found a clear relationship between the 3D display of the pharmacophores and biological activity. In particular, **6** showed good efficacy in inhibiting fibronectin adhesion to the $\alpha_v\beta_3$ integrin-expressing human melanoma cells SK-MEL-24 ($EC_{50} = 3.7 \times 10^{-7}$).
(© Wiley-VCH Verlag GmbH & Co. KGaA, 69451 Weinheim, Germany, 2008)

Introduction

Many biologically active peptides and proteins exert their functions by means of relatively small regions of their folded surfaces.[1] As a consequence, much effort has been dedicated to the design of smaller, conformationally defined peptides or analogs[2] that mimic these localized folded regions.[1,3]

Within the family of cyclic peptides, cyclotetrapeptides (CTPs) composed of all α-amino acids can be considered truly minimalist turn mimics,[4] but their potential utility in medicinal chemistry is often hampered by difficult synthesis and scarce conformational definition in a polar environment. On the other hand, the incorporation of a distinct β^3- or β^2-amino acid residue in the CTP sequence may result in the stabilization of the overall secondary structure.[4b,4c,5]

As a continuation of our recent investigations on the use of cyclic peptides and analogs as restricted mimics of biologically active, naturally occurring peptides,[6] we report the partially modified retro-inverso[7] CTP (PMRI–CTP) models c[βAla-ψ(NHCO)-Ala-ψ(NHCO)-Gly-Phe] (**1**), c[βAla-ψ(NHCO)-Ala-ψ(NHCO)-Gly-D-Phe] (**2**), c[βPhe-ψ(NHCO)-Ala-ψ(NHCO)-Gly-Phe] (**3**), c[βPhe-ψ(NHCO)-Ala-ψ(NHCO)-Gly-D-Phe] (**4**), and related compounds c[βAla-ψ(NHCO)-Asp-ψ(NHCO)-Gly-Arg] (**5**), c[βAla-ψ(NHCO)-Asp-ψ(NHCO)-Gly-D-Arg] (**6**) (Figure 1).

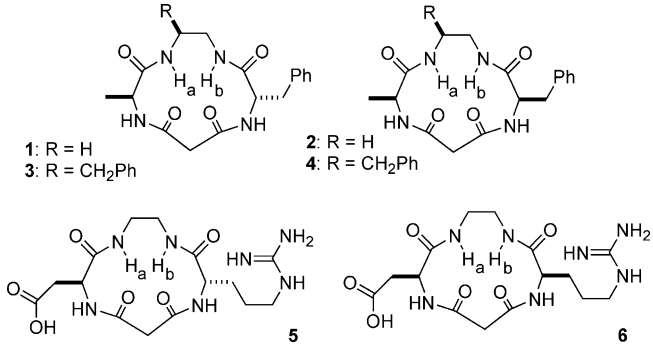

Figure 1. Structures of PMRI–CTPs **1**–**6**.

These 13-membered PMRI–CTPs containing a 1,2-diamine as a β-amino acid analog represent easily available CTP mimetics and show promising applications in medicinal chemistry and biochemistry as topologically defined scaffolds. Indeed, the low molecular weight, the increased lipophilicity, and the presence of modified peptide bonds is expected to improve the bioavailability and ADMET profile.[2]

[a] Department of Chemistry "G. Ciamician", University of Bologna,
Via Selmi 2, 40126 Bologna, Italy
Fax: +39-051209456
E-mail: luca.gentilucci@unibo.it
[b] Department of Pharmacology, University of Bologna,
Via Irnerio 42, 40126 Bologna, Italy
E-mail: spampi@biocfarm.unibo.it
Supporting information for this article is available on the WWW under http://www.eurjoc.org or from the author.

 © 2008 Wiley-VCH Verlag GmbH & Co. KGaA, Weinheim

Results and Discussion

Peptides **1**–**6** were easily obtained in a few steps by cyclization of the corresponding linear precursors obtained in turn by divergent synthesis in solution (see also Supporting Information).

As a representative example, the preparation of **3** (and **4**) is depicted in Scheme 1 (Experimental Section). Chiral Cbz-1,2-diamine **7** was obtained by reduction of Cbz-Phe-NH_2[8] with BH_3.[9] Coupling of **7** under standard conditions with Fmoc-Phe-OH, and deprotection of the resulting dipeptide by treatment with 2 M dimethylamine in THF afforded **8** in good yield. Dipeptide **9** was readily prepared from Meldrum's acid and NH_2-Ala-OBz. The coupling of dipeptides **8** and **9** gave the fully protected linear tetrapeptide. The removal of the protecting groups with H_2 and Pd/C, and finally cyclization with DPPA, gave cyclopeptide **3** in good yield and purity after semipreparative RP-HPLC.

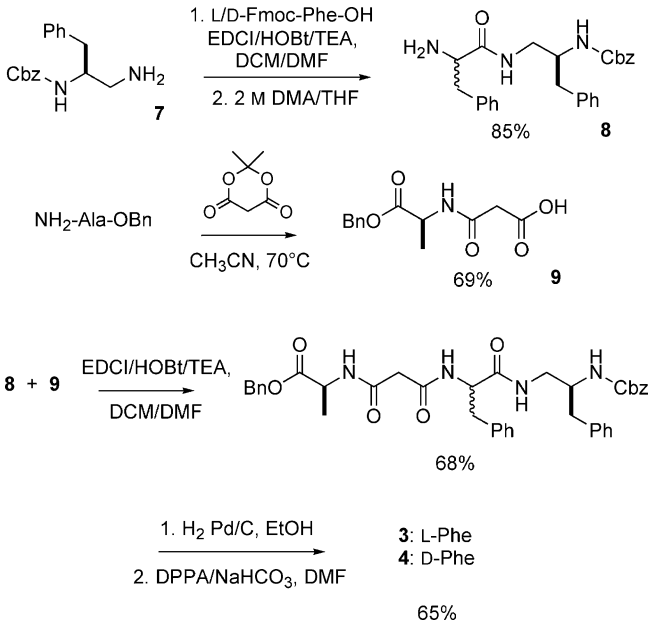

Scheme 1. Synthesis of PMRI–CTPs **3**, **4**.

The ^{1}H-NMR analysis of models **1**–**4** revealed a single set of resonances (Supporting Information). However, the amide protons generally showed modest $J_{NH,CH}$ values (<9 Hz), which suggests a fast equilibrium rather than complete conformational rigidity.[10]

Nevertheless, variable temperature (VT) ^{1}H-NMR analysis denoted that the NHa and NHb protons (Figure 1) appear to be involved in H-bonds ($|\Delta\delta/\Delta t|$ lower than or close to 1 ppb/K,[11] Table 1), which supports the existence of a population of ordered structures with definite secondary structural elements.

The conformational features of the PMRI–CTPs were investigated by spectroscopic and molecular dynamics (MD) analyses. We could not perform experiments in water, for the peptides were practically insoluble. Many peptides or peptidomimetics of interest described in the literature are not highly soluble in water and were studied experimentally in organic polar environments, in particular DMSO.[4b,4c,7f,12] Accordingly, the NMR experiments on lipophilic cyclopeptides **1**–**4** were performed at 400 MHz in [D_6]DMSO.

Table 1. $\Delta\delta/\Delta t$ values (ppb/K) of amide protons for **1**–**4**, **13**, **14**, as determined by VT-^{1}H-NMR analysis in [D_6]DMSO at 400 MHz over the range 298–348°K.[a]

Compound	AlaNH	L/D-PheNH	NHb[a]	NHa[a]
1	–5.0	–5.3	–0.05	–0.7
2	–4.4	–4.1	–0.5[b]	–1.3
3	–5.5[c]	–5.0[c]	–1.2	+1.4
4	–4.1	–3.0	–0.2	–1.3
	AspNH	L/D-ArgNH	NHb	NHa
13	–6.3	–5.7	–0.2	–1.5
14	–4.8	–4.9	–0.8	+0.6

[a] See Figure 1. [b] Determined by gCOSY experiments recorded at 298 and 313°K. [c] PheNH and AlaNH in **3** are superimposed.

The 2D-ROESY analysis furnished details on cyclopeptide backbone conformations (Supporting Information, Tables S1–S4). Apart from the inversion of configuration at Phe, the most significant difference between **1** and **2** (and between **3** and **4**) is limited to the L/D-PheNH region (Figure 3), as revealed by the comparison of the ROESY cross peaks between the $COCH_2CO$ protons and L/D-PheNH or AlaNH (Figure 2). In **1**, AlaNH is in close proximity of one of the two $COCH_2CO$ protons (at 3.2 ppm), whereas PheNH is close to the other (δ = 3.1 ppm). In **2**, both AlaNH and D-PheNH are close to the same $COCH_2CO$ proton (δ = 3.3 ppm), and D-PheNH shows also a medium intensity cross peak with the second $COCH_2CO$ (δ = 2.8 ppm). The behavior of **3** is similar to that of **1**, whereas the behavior of **4** reproduces that of **2**.

The occurrence of ROESY cross peaks between D-PheNH and both the $COCH_2CO$ protons, which should presumably occupy opposite sides of molecular plane, seems to suggest that in **2** and **4** D-PheNH could flip above and below the molecular plane.

Further, the existence in the ROESYs of **1** and **2** of strong cross peaks for NHb-PheNH and NHb-PheHα, and for NHa-AlaNH and NHa-AlaHα, is indicative that NHa and NHb (Figure 1) can flip above and below the backbone plane, as PheNH and PheHα, AlaNH and AlaHα are *trans* (Supporting Information, Tables S1–S4).

Low-energy conformations consistent with spectroscopic analyses were obtained by restrained MD by using the distances deduced from ROESY as constraints (see also Supporting Information). For both **1** and **2**, the computations gave different structures, each of which showed some violations of constraints. The structures having the lowest internal energy and the least number of violations are shown in Figure 3.

The structure proposed for **1** can be characterized by two inverse γ-turns, one centered on Phe (ϕ = –101, ψ = +51) and the other on Ala (ϕ = –98, ψ = +50), whereas the representative structure of **2** is roughly compatible with an inverse γ-turn centered on Ala (ϕ = –130, ψ = +68).

 © 2008 Wiley-VCH Verlag GmbH & Co. KGaA, Weinheim

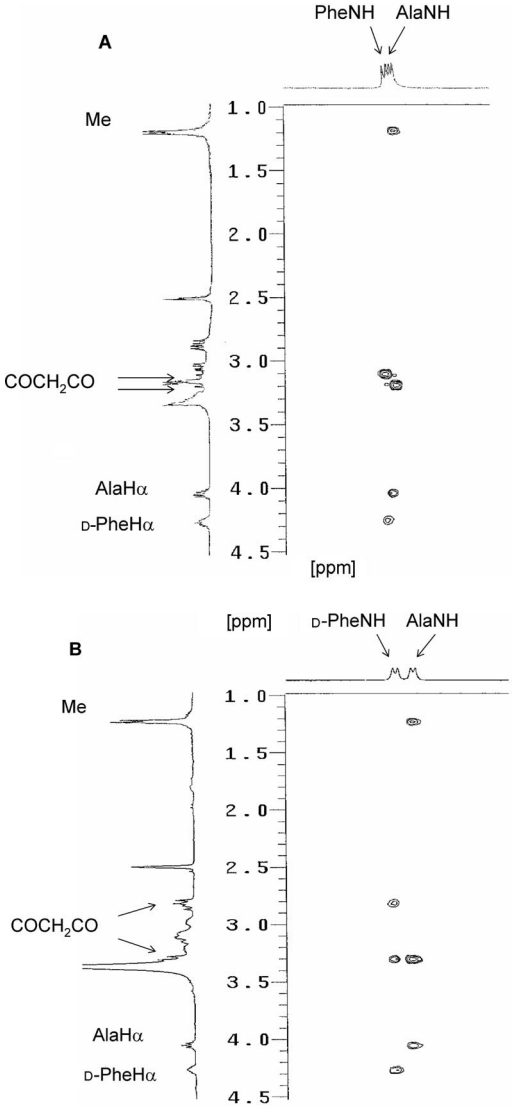

Figure 2. Inset of ROESY observed for **1** (A) and **2** (B) in [D_6]-DMSO at 400 MHz (room temp.) showing the cross peaks between $COCH_2CO$ and L/D-PheNH/AlaNH protons.

On the contrary, more than 90% of the structures of **3** calculated by restrained MD did not show any violation of restraints, and all were well ordered. Apparently, the introduction of a further substituent on the diamine is sufficient to confer upon the structure conformational homogeneity.

The representative structure of **3** in Figure 3 is compatible with a type I β-turn centered on Phe–diamine and a second one centered on Ala–diamine. However, this structure does not confirm the presence of H-bonds as predicted by VT-^{1}H-NMR analysis, probably for the occurrence of a fast equilibrium between slightly different geometries, whose average in the NMR timescale gives the NMR-derived structure.

In order to investigate the dynamic behavior of **3** in water to determine the eventual secondary structures stabilized by H-bonds, unrestrained MD simulations were conducted in a box of explicit water molecules for 5.0 ns by using the

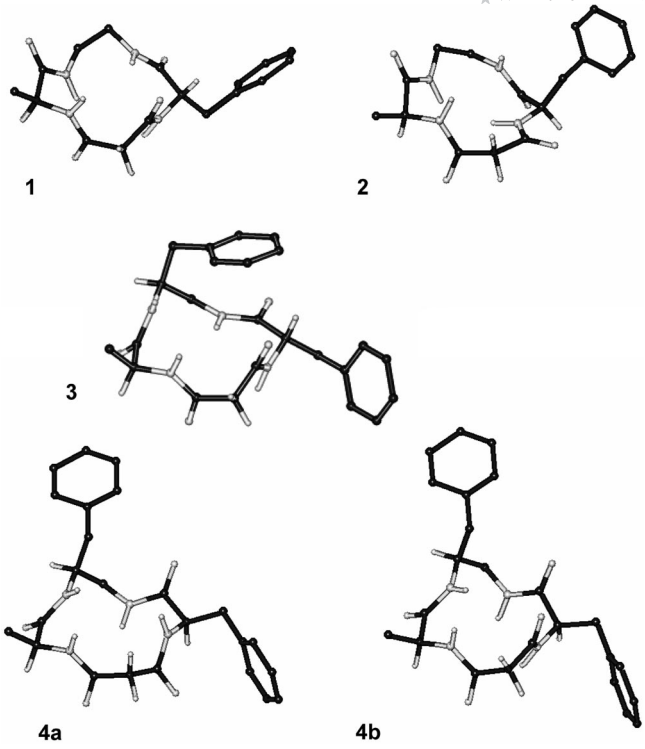

Figure 3. Representative lowest-energy structures of **1**–**4** calculated by restrained MD with the least number of violations of ROESY data (Supporting Information).

NMR-derived geometry as a starting structure. During this period, the analysis of the trajectories showed modest backbone flexibility (Figure 4).

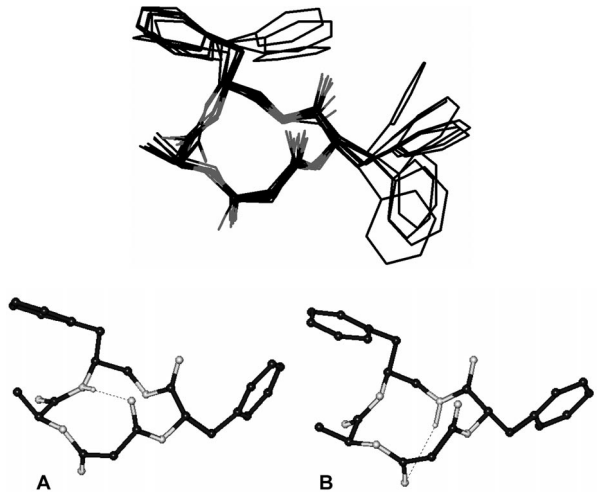

Figure 4. Overlay of minimized structures of **3** sampled every 500 ps during the unrestrained 5.0 ns MD simulation in explicit water, and representative structures **A**, **B** characterized by explicit H-bonds and secondary structural elements.

Moreover, the simulation clearly revealed the occurrence of backbone structures **A** and **B** with NHa and NHb alternatively participating in explicit H-bonds (Figure 4). The dihedral angles of Phe–diamine (for **A**: ϕ_{i+1} = –54, ψ_{i+1} = –40, ϕ_{i+2} = –96, ψ_{i+2} = –28; for **B**: ϕ_{i+1} = –83, ψ_{i+1} = –38,

 © 2008 Wiley-VCH Verlag GmbH & Co. KGaA, Weinheim

ϕ_{i+2} = –92, ψ_{i+2} = –37), and Ala–diamine (for **A**: ϕ_{i+1} = –65, ψ_{i+1} = –33, ϕ_{i+2} = –116, ψ_{i+2} = –28; for **B**: ϕ_{i+1} = –73, ψ_{i+1} = –29, ϕ_{i+2} = –89, ψ_{i+2} = –37) fragments are consistent with two symmetric type I β-turns,[4b,4c] although only the latter fragment can be considered a realistic type I β-turn mimic, for the position of the benzyl group.

Concerning **4**, restrained MD essentially gave two families of structures, represented by **4a** and **4b** (Figure 3), with nearly the same energy, differing exclusively in the opposite orientation of D-PheNH.

Both **4a** and **4b** are compatible with a type I β-turn centered on the Ala–diamine fragment, but **4b** also shows a type I β-turn on the Phe–diamine moiety. The two structures reasonably represent distinct conformers in equilibrium.

However, **4b** shows a smaller number of distance violations, and a structure more compatible with VT-NMR spectroscopic data, which are suggestive of two H-bonds on NHa and NHb.

Unrestrained MD simulations performed on **4a** evidenced the formation of a single explicit H-bond involving NHb, whereas unrestrained MD performed on **4b** showed the occurrence of H-bonds involving NHa and/or NHb (Figure 5). The simulations failed to reproduce the inversion of D-PheNH; evidently, this rotation is slow relative to the time selected for the simulation (5.0 ns).

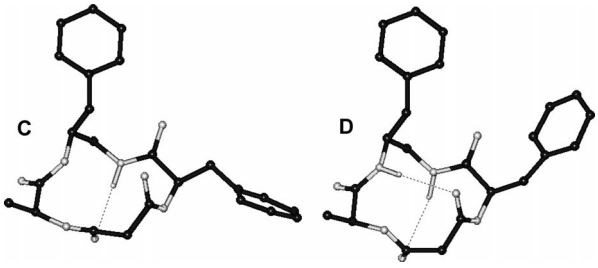

Figure 5. Representative structures **C**, **D** of **4b** calculated by unrestrained MD, characterized by explicit H-bonds and secondary structural elements.

Overall, the conformational analysis of **1**–**4** revealed that the PMRI–CTPs containing an unsubstituted diamine show some flexibility, especially in the diamine region, whereas the PMRI–CTPs that contain a substituted diamine are conformationally much more stable. On the other hand, the 3D display of the side chains is well-defined for all the models.

This observation is not unexpected; for instance, it has been well documented that cyclic penta- or hexapeptides can adopt defined 3D structures and clear side-chain positions, depending on the amino acid stereochemistry, but the presence of a glycine unit generally introduces a fast local backbone switch.[10,13]

The cyclic structures described constitute distinct, alternative 13-membered scaffolds with respect to those composed of α-amino acids plus a β-residue (see Introduction).

For instance, peptidomimetic **3**, c[βPhe-ψ(NHCO)-Ala-ψ(NHCO)-Gly-Phe], can be considered a PMRI analog of the recently reported CTP containing a β^2-amino acid c[(*S*)-β^2hPhe-D-Pro-Lys-Phe][5a] (**E**, Figure 6). In normal cyclopeptides, the 3D structure is generally determined for the most part by the specific array of the stereogenic centers, whereas the nature of the residues is less important.[10,13]

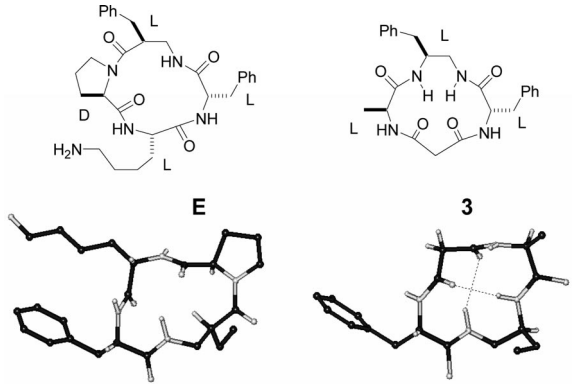

Figure 6. Comparison of the backbones of representative structures of c[βPhe-ψ(NHCO)-Ala-ψ(NHCO)-Gly-Phe] (**3**) and c[(*S*)-β2hPhe-D-Pro-Lys-Phe] **E** (some side chains have been omitted for clarity).

Peptides **3** and **E** share a common stereochemistry pattern. The (*S*)-diamine residue in **3** matches the (*S*)-β^2Phe in **E**; the L configuration of Ala in partially retro-inverso **3** corresponds to the D configuration of Pro in the normal peptide; the malonyl moiety, ψ(NHCO)-Gly, can act as a D-amino acid; and the last residue is the same for **3** and **E**. Comparison of the two structures proves that the two scaffolds show distinct features (Figure 6), in particular for the presence of a *cis* β-Phe-D-Pro ω bond in **E**, and for the position of the β-Phe side chain, which in **E** is placed below the plane, whereas in **3** it remains above.

Finally, in order to validate the structural deductions based on spectroscopic and MD analyses, we made a preliminary test of the potential utility of the PMRI–CTP scaffolds in medicinal chemistry. We observed that the main structural difference between **1** and **2**, and between **3** and **4**, is the distance between the β carbons of Ala and L/D-Phe; for example this distance is 8.4 Å in **1** and 7.6 Å in **2**. The latter value nicely fits the requisites generally accepted for the antagonists of $\alpha_v\beta_3$ integrins. Peptidomimetic antagonists based on cyclic cores carrying a guanidino and carboxylic-type functionality have been very often adopted for investigating how the 3D side chains affect biological activity.[4b,4c,13] In particular, it was exhaustively demonstrated that a comparatively short distance between the β carbons (7–8 Å) favored selective binding to $\alpha_v\beta_3$ integrins over other RGD-binding integrins.[13] Furthermore, different additional lipophilic flanking groups[14] at the N- and C-terminus very often proved to be crucial for high affinity and selectivity.[15] To avoid any effect of such flanking groups, we synthesized RGD mimetics **5** and **6**, which are based on the structures of **1** and **2**, containing the unsubstituted diamine, and we assayed their biological activity as integrin inhibitors. The lack of full rigidity does not constitute a insurmountable impediment in terms of biological activity,

 © 2008 Wiley-VCH Verlag GmbH & Co. KGaA, Weinheim

for the side-chain topology with respect to the peptide bond orientation is of higher relevance.[5b,13c,13e]

The structural analysis of **13** and **14**, which are the fully protected precursors of **5** and **6** (Supporting Information, Tables S5 and S7), gave unexpected results. Comparison of the ^{1}H NMR, VT-NMR, and ROESY analyses indicated that although **1** and **13** are structurally analogous, **2** [L-Ala^1, D-Phe^3] and **14** [L-Asp^1, D-Arg^3] differ in the mirror disposition of the backbone (see Figures 3 and 7). In particular, in **2** the residue having its NH positioned on the molecular plane has the D configuration, whereas in **14** the NH that lies on the molecular plane belongs to the L residue. Apart from this difference, the expected distance between the β carbon atoms is retained.

Figure 7. Representative structures of **13** and **14** calculated by restrained MD with the lowest internal energy and the least number of violations of ROESY data (*t*Bu and Mtr protective groups have been omitted for clarity).

To evaluate the potential activity of **5** and **6** as $\alpha_v\beta_3$ integrin inhibitors, we tested their ability to inhibit the adhesion of an $\alpha_v\beta_3$ integrin-expressing cell line, SK-MEL-24, to the specific ligand fibronectin.[16] Fibronectin was immobilized on each well of a 96-assay plate. SK-MEL-24 cells were preincubated with various peptide concentrations, and dispensed on the wells. After removal of nonadherent cells, the number of adherent cells was quantified by fluorometry. The activity of potential antagonists was determined by the number of cells adhered relative to the control.

RGD mimetics **5** and **6** showed IC_{50} values of 5×10^{-4} and 3.7×10^{-7} M, respectively. The inhibitory activity displayed by **6** is attractive,[16] and the different performance of **5** seems to confirm that in **6** the pharmacophores actually adopt spatial positions compatible with an efficient ligand–receptor interaction, which substantiates the structures proposed on the basis of spectroscopic and computational analyses.

Conclusions

The easily available PMRI–CTPs constitute a novel kind of 13-membered cyclotetrapeptide β-turn mimics. The introduction of the retro modification by insertion of a substituted 1,2-diamine and a diacid induced a peculiar backbone conformation. This conformation can be an alternative to that of cyclotetrapeptides containing a normal sequence of amino acids. Therefore, the PMRI–CTPs can find applications as effective scaffolds for designing biologically active molecules with a predictable, atypical 3D display of the pharmacophores, which is useful for spatial screening of diverse bioactive conformations.

In addition, the retro-peptide bonds can be regarded as true peptide-bond surrogates. The presence of these modified peptide bonds is expected to increases the biological half lives of the compounds. Further, the cyclic structure and the presence of intramolecular H-bonds increase the molecular lipophilicity. The combination of increased stability and increased lipophilicity can strongly impact the overall bioavailability of compound based on PMRI–CTP scaffolds.

Experimental Section

General Methods: Unless stated otherwise, standard chemicals were obtained from commercial sources and used without further purification. The SK-MEL-24 cell line (human malignant melanoma) was obtained from the American Tissue Type Collection (ATCC); BSS from Invitrogen; fetal bovine serum from Cambrex; essential medium from Eagle; PBS from Cambrex; Fibronectin (FN) from Sigma–Aldrich. Flash chromatography was performed on silica gel (230–400 mesh) with mixtures of distilled EtOAc and MeOH. Analytical RP-HPLC was performed with an ODS column, 4.6-μm particle size, 100 Å pore diameter, 250 mm, DAD 210 nm, with H_2O/CH_3CN (9:1→2:8) in 20 min at a 1.0 mL min^{-1} flow, followed by 10 min at the same composition. Semipreparative RP-HPLC was performed on a C18 column, 7-μm particle size, 21.2 × 150 mm, from H_2O/CH_3CN (9:1→3:7) in 15 min at a 12 mL min^{-1} flow. Fluorometry to evaluate the number of adherent cells was performed with a multilabel counter.

^{1}H NMR spectra were recorded by using 5-mm tubes by using 0.01 M peptide at room temperature. Chemical shifts are reported as δ values relative to the solvent peak. VT-^{1}H-NMR experiments were performed over the range 298–348°K. 2D spectra were acquired in the phase-sensitive mode and processed by using a 90° shifted, squared sine-bell apodization. ^{1}H-NMR resonances were assigned from gCOSY and ROESY spectra. gCOSY experiments were recorded with a proton spectral width of 3103 Hz. ROESY experiments were recorded with a 300 ms mixing time with a proton spectral width of 3088 Hz.

Representative Procedure for the Synthesis of PMRI–CTPs: Compound **3** was prepared by cyclization of the corresponding linear precursor (Scheme 1), obtained in turn by in solution coupling of dipeptides **8** and **9**.

Benzyl [2-(2-Amino-3-phenylpropionylamino)-1-benzylethyl]carbamate (8): HOBt (0.16 g, 1.2 mmol) was added to a stirred solution of Fmoc-Phe-OH (0.39 g, 1.0 mmol) in DCM/DMF (9:1, 15 mL) at room temp. After 10 min, **7**[8,9] (0.28 g, 1.0 mmol), EDCI·HCl salt (0.24 g, 1.2 mmol), and TEA (0.40 mL, 3.0 mmol) were added while stirring at room temp. After 4 h, the mixture was diluted with DCM, and the solution was washed with HCl (0.5 M), and a saturated aqueous solution of Na_2CO_3. The organic layer was dried with Na_2SO_4, and the solvent was removed under reduced pressure. The dipeptide was isolated by crystallization from DCM/Et_2O (85%). Fmoc-group deprotection was performed by treatment with 5 mL of 2 M dimethylamine in THF at room temp. After 20 min the solution was evaporated under reduced pressure, and the treatment was repeated. After final evaporation of the solution, the residue was triturated twice with *n*-pentane. Crude **8** (0.36 g, 85%, 83% pure by RP-HPLC) was used without further purification. MS (ES): *m*/*z* = 431.1 [M + 1].

Benzyl 2-(2-Carboxyacetylamino)propionate (9): A solution of Meldrum's acid (0.85 g, 6 mmol) and NH_2-Ala-OBz (0.90 g, 5 mmol)

 © 2008 Wiley-VCH Verlag GmbH & Co. KGaA, Weinheim

in CH_3CN (10 mL) was warmed to 70 °C under an inert atmosphere. After 5 h, cyclohexane/Et_2O (4:1, 40 mL) was added, and the oily residue that precipitated was separated. This residue was washed with a hexane/Et_2O mixture (4:1, 2 × 20 mL), and the resulting dense oil was diluted with EtOAc (40 mL) and washed with HCl (0.1 M, 2 × 5 mL). The organic layer was dried with Na_2SO_4, and the solvent was evaporated under reduced pressure (temp. <40 °C) to give **9** as a waxy solid, which was used for the following step without further purification (0.91 g, 69%, 80% pure by NMR analysis). ^{1}H NMR (300 MHz, [D_6]DMSO): δ = 1.40 (d, J = 7.2 Hz, 3 H, CH_3), 3.40 (s, 2 H, $COCH_2CO$), 4.59–4.66 (m, 1 H, AlaHα), 5.20 (s, 2 H, CH_2Ph), 7.25–7.41 (m, 5 H, Ph), 7.80 (br. d, 1 H, NH), 9.40–10.1 (br. s, 1 H, COOH) ppm.

c[βPhe-ψ(NHCO)-Ala-ψ(NHCO)-Gly-Phe] (3): Dipeptides **9** (0.13 g, 0.5 mmol) and **8** (0.22 g, 0.5 mmol) were coupled under the same conditions used for the synthesis of **8** in the presence of HOBt (0.082 g, 0.6 mmol), EDCI·HCl salt (0.12 g, 0.6 mmol), and TEA (0.20 mL, 1.5 mmol), in DCM/DMF (9:1, 10 mL) at room temp. After 6 h, the usual workup afforded the protected tetrapeptide, which was isolated by crystallization from DCM/Et_2O (0.23 g, 68%, 86% pure by RP-HPLC). MS (ES): m/z = 679.2 [M + 1].

Protecting group removal was performed by treatment with H_2 and cat. Pd/C in EtOH (10 mL) at room temp. After 6 h, the mixture was filtered through Celite, and the solvent was evaporated under reduced pressure to give the deprotected linear tetrapeptide (0.15 g, 96%, 82% pure by RP-HPLC), which was used without further purification. MS (ES): m/z = 454.2 [M + 1].

Peptide Cyclization: A mixture of the deprotected tetrapeptide (0.15 g, 0.32 mmol), DPPA (0.15 mL, 0.68 mmol), and $NaHCO_3$ (0.43 g, 5.1 mmol) in DMF (70 mL) was stirred at room temp. After 48 h, the solvent was distilled at reduced pressure, the residue was diluted with water, and the mixture was extracted three times with DCM. The solution was evaporated at reduced pressure, and the residue was precipitated from DCM/Et_2O. Semipreparative RP-HPLC gave **3** (0.092 g, 68%, 95% pure by RP-HPLC). ^{1}H NMR (400 MHz, [D_6]DMSO): δ = 1.03 (d, J = 7.2 Hz, 3 H, CH_3), 2.57 (dd, J = 10.0, 14.0 Hz, 1 H, PhCH_2CHNHa), 2.75 (dd, J = 5.6, 14.0 Hz, 1 H, PhCH_2CHNHa), 2.89 (dd, J = 8.7, 15.0 Hz, 1 H, PheHβ), 2.94–3.11 (m, 2 H, NHbCH_2), 3.09 (dd, J = 3.6, 15.0 Hz, 1 H, PheHβ), 3.13 (d, J = 10.3 Hz, 1 H, $COCH_2CO$), 3.17 (d, J = 10.3 Hz, 1 H, $COCH_2CO$), 3.86 (dq, J = 5.7, 7.3 Hz, 1 H, AlaHα), 3.88–3.98 (m, 1 H, NHaCH), 4.30–4.39 (m, 1 H, PheHα), 6.16 (d, J = 8.4 Hz, 1 H, NHa), 6.82 (br. t, 1 H, NHb), 7.03–7.16 (m, 10 H, ArH), 9.00 (d, J = 6.0 Hz, 2 H, PheNH + AlaNH) ppm. MS (ES): m/z = 437.1 [M + 1].

Conformational Analysis: The restrained MD simulations were conducted by using AMBER[17] force field with a distance dependent ε = 4.0xr. A 50-ps simulation at 1200°K was used for generating 100 random structures that were subsequently subjected to a 20 ps restrained MD with a 50% scaled force field at the same temperature, followed by 20 ps with full restraints (distance force constant: 7 kcal mol^{-1} Å^{-2}), after which the system was cooled in 5 ps to 50°K. For the absence of Hα-COCH_2CO or Hα-NHCH (i, i + 1) ROESY cross peaks, the ω bonds were set at 180° (force constant: 16 kcal mol^{-1} Å^{-2}). Only ROESY-derived constraints were included in the restrained molecular dynamics. H-bond interactions were not included as well as torsion angle restraints. ROESY intensities were classified according to a calibration against the intensity of geminal protons. Very strong, strong, medium, and weak signals were associated to distances of 2.3, 2.6, 3.0, and 4.0 Å, respectively. Geminal couplings and other obvious correlations were discarded. The resulting structures were minimized with 3000 cycles of steepest descent and 3000 cycles of conjugated gradient (convergence: 0.01 kcal mol^{-1} Å^{-1}). The structures that showed the lowest internal energy and the least number of violations of the experimental data were selected and analyzed.

MD simulation in explicit water was performed for 5.0 ns at 298°K by using the AMBER force field in a 30×30×30 Å box of standard TIP3P models of equilibrated water,[18] with a minimum solvent–solute distance of 2.3 Å, at constant temperature and pressure (Berendsen Scheme,[19] bath relaxation constant 0.2).

Cell Adhesion Assays

Inhibition of the Adhesion of an $\alpha_v\beta_3$ Integrin-Expressing Cell Line, SK-MEL-24, to Fibronectin: As a reference compound we tested the $\alpha_v\beta_3$ integrin antagonist AcDRGDS, which showed an IC_{50} of 0.2×10^{-7} M.[16]

Experimental Details: SK-MEL-24 cells were routinely grown as adherent monolayers in minimum essential medium in Earle's BSS supplemented with 10% fetal bovine serum, nonessential amino acids and 1 mM sodium pyruvate in a humidified environment containing 5% CO_2 and 95% air at 37 °C.

Assays were performed as described in the literature,[16] with the following modifications. Cells were harvested with 0.05% trypsin/0.53 mM EDTA and washed three times with 0.5 mg mL^{-1} trypsin inhibitor in PBS. The final cell pellet was resuspended at a concentration of 10^6 cells per mL in PBS. FN was diluted in PBS (10 μg mL^{-1}) and 100 μL of this solution was added to each well of a 96-assay plate and incubated for 2 h at 37 °C. The wells were aspirated and washed once with PBS. Wells were blocked with 100 μL of 1% BSA in MEM for 1 h at 37 °C and washed once with PBS. Cells were preincubated with various concentrations of peptides **5**, **6** for 30 min at room temp. agitating, and 50 μL of this suspension were added to FN-coated wells (in quadruplicate). The plate was incubated for 90 min at room temp. Following the incubation period, the wells were aspirated and washed three times (or until no more cells were seen in the background wells) with PBS. The number of cells attached was determined by a hexosaminidase reaction.[20] Hexosaminidase substrate (*p*-nitrophenol-*N*-acetyl-β-D-glucosaminide; 50 μL, at 7.5 mM in 0.1 M citrate buffer, pH = 5, mixed with an equal volume of 0.5% triton X-100 in water) was added to each well. The plate was incubated 1 h at 25 °C followed by addition of 100 μL stopping solution (50 mM glycine buffer, pH = 10.4, containing 5 mM EDTA). Standard curves prepared by adding a different number of cells were run in parallel in the same plate. The number of adherent cells was quantified by fluorometry. The activity of potential antagonists was determined by the number of cell adhered relative to the control. Aliquots of this suspension were added to fibronectin-coated wells. The concentration–response curves were analyzed by a least-square curve-fitting computer program and IC_{50} values were determined (GraphPad, San Diego, CA, USA).

Supporting Information (see footnote on the first page of this article): Syntheses of the cyclopeptides, NMR characterization, and conformational analyses.

Acknowledgments

We gratefully thank MIUR (Ministero dell'Università e della Ricerca), Bologna University, and Fondazione CARISBO (Cassa di Risparmio in Bologna), Bologna, for providing financial support. We also thank A. Garelli, Dr. E. Florio, and Dr. R. Artali.

 © 2008 Wiley-VCH Verlag GmbH & Co. KGaA, Weinheim

[1] a) J. D. A. Tyndall, B. Pfeiffer, G. Abbenante, D. P. Fairlie, *Chem. Rev.* **2005**, *105*, 793–826; b) V. J. Hruby, P. M. Balse, *Curr. Med. Chem.* **2000**, *7*, 945–970.

[2] a) V. J. Hruby, R. S. Agnes, *Biopolymers* **2000**, *51*, 391–410; b) for a recent review on the use of peptidomimetics in biochemistry, medicine, pharmacology, etc., see: L. Gentilucci, A. Tolomelli, F. Squassabia, *Curr. Med. Chem.* **2006**, *13*, 2449–2466.

[3] A. Carotenuto, A. M. D'Ursi, B. Mulinacci, I. Paolini, F. Lolli, A. M. Papini, E. Novellino, P. Rovero, *J. Med. Chem.* **2006**, *49*, 5072–5079.

[4] a) N. Loiseau, J.-M. Gomis, J. Santolini, M. Delaforge, F. Andre, *Biopolymers* **2003**, *69*, 363–385; b) F. Schumann, A. Muller, M. Koksch, G. Muller, N. Sewald, *J. Am. Chem. Soc.* **2000**, *122*, 12009–12010; c) M. P. Glenn, M. J. Kelso, J. D. A. Tyndall, D. P. Fairlie, *J. Am. Chem. Soc.* **2003**, *125*, 640–641, and references herein; d) P. Mora, C. Mas-Moruno, S. Tamborero, L. J. Cruz, E. Perez-Paya, F. Albericio, *J. Pept. Sci.* **2006**, *12*, 491–496.

[5] a) A. S. Norgren, F. Buttner, S. Prabpai, P. Kongsaeree, P. I. Arvidsson, *J. Org. Chem.* **2006**, *71*, 6814–6821; b) N. Maulucci, M. G. Chini, S. Di Micco, I. Izzo, E. Cafaro, A. Russo, P. Gallinari, C. Paolini, M. C. Nardi, A. Casapullo, R. Riccio, G. Bifulco, F. De Riccardis, *J. Am. Chem. Soc.* **2007**, *129*, 3007–3012.

[6] a) G. Cardillo, L. Gentilucci, A. Tolomelli, R. Spinosa, M. Calienni, A. R. Qasem, S. Spampinato, *J. Med. Chem.* **2004**, *47*, 5198–5203; b) F. Benfatti, G. Cardillo, S. Fabbroni, L. Gentilucci, R. Perciaccante, A. Tolomelli, M. Baiula, S. Spampinato, *Tetrahedron: Asymmetry* **2006**, *17*, 167–170; c) L. Gentilucci, F. Squassabia, R. Artali, *Curr. Drug Targets* **2007**, *8*, 185–196.

[7] a) M. Chorev, M. Goodman, *Acc. Chem. Res.* **1993**, *26*, 266–273; b) M. D. Fletcher, M. M. Campbell, *Chem. Rev.* **1998**, *98*, 763–795; c) M. Chorev, *Biopolymers* **2005**, *80*, 67–84; d) Y. S. Lee, R. S. Agnes, P. Davis, S.-w. Ma, H. Badghisi, J. Lai, F. Porreca, V. J. Hruby, *J. Med. Chem.* **2007**, *50*, 165–168; e) K.-J. Kim, S.-W. Park, S. S. Yoon, *J. Kor. Chem. Soc.* **2000**, *44*, 286–289; f) for the use of a 10-membered ethylene-bridged PMRI peptide as β-turn mimetic, see: Y. Han, C. Giragossian, D. F. Mierke, M. Chorev, *J. Org. Chem.* **2002**, *67*, 5085–5097.

[8] S. Nakabayashi, C. D. Warren, R. W. Jeanloz, *Carbohydr. Res.* **1988**, *174*, 279–289.

[9] T. Morie, S. Kato, H. Harada, I. Fujiwara, K. Watanabe, J.-I. Matsumoto, *J. Chem. Soc. Perkin Trans. 1* **1994**, 2565–2569.

[10] a) S. J. Stradley, J. Rizo, M. D. Bruch, A. N. Stroup, L. M. Gierasch, *Biopolymers* **1990**, *29*, 263–287; b) H. Kessler, *Angew. Chem. Int. Ed. Engl.* **1982**, *21*, 512–523.

[11] C. Toniolo, *CRC Crit. Rev. Biochem.* **1980**, *9*, 1–44.

[12] For a leading reference on the use of DMSO as a biomimetic medium, see: P. A. Temussi, D. Picone, G. Saviano, P. Amodeo, A. Motta, T. Tancredi, S. Salvadori, R. Tomatis, *Biopolymers* **1992**, *32*, 367–372. For other selected examples of recently published papers, see: a) J. Chatterjee, D. Mierke, H. Kessler, *J. Am. Chem. Soc.* **2006**, *128*, 15164–15172; b) E. Locardi, D. G. Mullen, R.-H. Mattern, M. Goodman, *J. Pept. Sci.* **1999**, *5*, 491–506; c) H. B. Lee, M. Pattarawarapan, S. Roy, K. Burgess, *Chem. Commun.* **2003**, *14*, 1674–1675.

[13] a) C. Henry, N. Moitessier, Y. Chapleur, *Mini-Rev. Med. Chem.* **2002**, *2*, 531–542; b) M. A. Dechantsreiter, E. Planker, B. Matha, E. Lohof, G. Holzemann, A. Jonczyk, S. L. Goodman, H. Kessler, *J. Med. Chem.* **1999**, *42*, 3033–3040; c) R. Haubner, R. Gratias, B. Diefenbach, S. L. Goodman, A. Jonczyk, H. Kessler, *J. Am. Chem. Soc.* **1996**, *118*, 7461–7472; d) K. Burgess, D. Lim, S. A. Mousa, *J. Med. Chem.* **1996**, *39*, 4520–4526; e) G. Casiraghi, G. Rassu, L. Auzzas, P. Burreddu, E. Gaetani, L. Battistini, F. Zanardi, C. Curti, G. Nicastro, L. Belvisi, I. Motto, M. Castorina, G. Giannini, C. Pisano, *J. Med. Chem.* **2005**, *48*, 7675–7687.

[14] M. Gurrath, G. Muller, H. Kessler, M. Aumailley, R. Timpl, *Eur. J. Biochem.* **1992**, *210*, 911–921.

[15] B. Cacciari, G. Spalluto, *Curr. Med. Chem.* **2005**, *12*, 51–70.

[16] a) S. Caltabiano, W. T. Hum, G. J. Attwell, D. N. Gralnick, L. J. Budman, A. M. Cannistraci, F. J. Bex, *Biochem. Pharm.* **1999**, *58*, 1567–1578; b) H. Fujii, H. Komazawa, H. Mori, M. Kojima, I. Itoh, J. Murata, I. Azuma, I. Saiki, *Biol. Pharm. Bull.* **1995**, *18*, 1681–1688.

[17] W. D. Cornell, P. Cieplak, C. I. Bayly, I. R. Gould, K. M. Merz, D. M. Ferguson, D. C. Spellmeyer, T. Fox, J. W. Caldwell, P. A. Kollman, *J. Am. Chem. Soc.* **1995**, *117*, 5179–5197.

[18] W. L. Jorgensen, J. Chandrasekhar, J. Madura, R. W. Impey, M. L. Klein, *J. Chem. Phys.* **1983**, *79*, 926–933.

[19] H. J. C. Berendsen, J. P. M. Postma, W. F. van Gunsteren, A. DiNola, J. R. Haak, *J. Chem. Phys.* **1984**, *81*, 3684–3690.

[20] U. Landegren, *J. Immunol. Methods* **1984**, *67*, 379–388.

Received: October 1, 2007
Published Online: November 28, 2007

 © 2008 Wiley-VCH Verlag GmbH & Co. KGaA, Weinheim